Brazilian Journal of Geophysics 41 (2023), 1, 17-32
Brazilian Geophysical Society
ISSN 2764-8044
DOI: 10.22564/brjg.v41i1.2205

HIGH RESOLUTION GAMMA-RAY SPECTROMETRY LOGGING APPLIED IN THE INTERPRETATION OF SEDIMENTARY PROCESSES AND ENVIRONMENTS OF THE ITARARÉ GROUP (PERMO-CARBONIFEROUS), PARANÁ BASIN, SANTA CATARINA STATE

André Dorival Miranda [1*], Marivaldo dos Santos Nascimento [1], Neivaldo Araújo de Castro [1], João Pedro Baesso [1], and Patrícia da Rocha M. N. Balistieri [2]

[1]Universidade Federal de Santa Catarina – UFSC, Florianópolis, SC, Brazil
[2]Fundação Universidade Regional de Blumenau – FURB, Blumenau, SC, Brazil

*Corresponding author e-mail: a.miranda@ufsc.br

ABSTRACT. Outcrop gamma-ray spectrometric logging in the upper strata of the Campo Mourão Formation and lower strata of the Taciba Formation were used to investigate: (i) the influence of lithological variation on gamma-ray patterns; (ii) its potential to discriminate and identify lithotypes; and (iii) sedimentary processes and related environments of these Permo-Carboniferous strata. The gamma-ray logs were subdivided into three gamma-ray units, according to the total count, concentrations and contents of K, eU and eTh. These gamma-ray units were associated to three depositional units: Glaciolacustrine system with thin-bedded turbidites in the Campo Mourão Formation; and two submarine fan systems (channels, overbanks and lobes) with thick-bedded turbidite systems in the Taciba Formation. Gamma-ray spectrometry allowed distinguishing 'common' shales from black shales, which are often similar in the faciological description in fieldwork. Likewise, carbonate levels were identified as a function of the decrease in gamma-ray concentrations in black shales of the Campo Mourão Formation. The relationship between the radiometric data and the grain size indicated that, in the field, the lithological heterogeneity has a great influence on the ability of the gamma-ray spectrometer to distinguish lithotypes. The eTh/K and eTh/eU ratios were used to infer sedimentary processes and related environments. Through the eTh/eU ratio, a reducing environment, responsible for the precipitation of authigenic uranium in low sedimentation rate depositional system, was evidenced, discriminating depositional units from different environments.

Keywords: gamma-ray spectrometry, sedimentary sequence, Paraná basin, stratigraphy, Gondwana.

INTRODUCTION

The Paraná Basin is a wide sedimentary cover with approximately 1.600.000 km² and has six sedimentary supersequences (Milani, 2004; Figure 1a). The Itararé Group (from Gondwana I Supersequence) has long been studied based on faciological and stratigraphic (Schneider et al., 1974; França and Potter, 1988; Vesely and Assine, 2006; d'Ávila, 2009; Neves et al., 2019), ichnological (Noll and Netto, 2018), and geophysical data (Costa et al., 2018). Some of these studies investigated the relationship between depositional aspects and the petrophysical properties of these deposits using data from wells and outcrops (e.g., França and Potter, 1988; Vesely, 2006; 2007). However, the available literature of the Itararé Group lacks in studies of gamma-ray spectrometry in outcrops.

Gamma-ray spectrometry (GRS) research in outcrops stems from the potentiality to identify subtle trends in gamma-ray logs associated with particularities of lithological successions (Bessa, 1995). Potassium (K), thorium (eTh) and uranium (eU) concentrations in the sampled rocks are recorded in gamma-ray spectral readings (Rider, 1996) and can be interpreted in the light of knowledge of depositional and geochemical processes.

In addition to the considerations extracted from the total count (TC) of gamma radiation, it is also relevant the ones that can be made taking into account the variations of the individualized spectra of potassium, thorium and uranium, and also between their eTh/K, eTh/eU and eU/K ratios (Basu et al., 2009).

In this paper, the GRS was used to investigate sedimentary processes and environments, as well as the influence of lithological variation on gamma-ray patterns and the potential to discriminate and identify lithotypes from the Campo Mourão Formation (Lontras Member) and Taciba Formation (Rio Segredo Member) exposed in the Presidente Getúlio and Doutor Pedrinho regions (Figure 1b). According to Schneider et al. (1974), the Itararé Group was divided into the Campo do Tenente, Mafra and Rio do Sul formations. França and Potter (1988), however, considering cycles of advance and retreat of the glaciers, divided this Group into the Lagoa Azul, Campo Mourão and Taciba Formations (Buso et al., 2019). The Campo Mourão Formation (CMF) consists of an ascending thinning cycle composed of sandstone, shale and siltstone; however, in the study area (Figure 1b), only the upper part of the formation known as Lontras Member/Shale (Castro, 1999) occurs and was deposited in proglacial context. According to d'Àvila (2009), dropstones at some stratigraphic levels indicate the advance and retreat of glaciers that released the clasts with the melting of icebergs, confined to depressions or paleovalleys, more pronounced to the south and wider and smoother in the *Doutor Pedrinho* region. In this region, the Taciba Formation (TF) is in contact with the CMF or lies in nonconformity on the Santa Catarina Granulitic Complex.

Close to the study area, the TF was interpreted as deltaic deposits accumulated in periglacial systems sometimes deposited directly on the granites of the *Dom Feliciano* Belt (Menezes and Nascimento, 2015; Zielinsk and Nascimento, 2015). The detrital composition of the sandstones of the Rio Segredo Member indicates an inland and transitional craton provenance, attributed to the *Dom Feliciano* Belt and the Luís Alves Craton (Menezes and Nascimento, 2015). Gamma-ray spectrometric relationships suggest an arid and cold climate during the deposition of the base of this formation (Costa et al., 2018).

THEORY AND METHODS

Gamma-ray spectrometry is an analytical technique used to identify and estimate the concentration of nuclides[1] that emit gamma radiation[2], known as radionuclides, by discriminating the energy levels of radiation from the researched targets. Gamma radiation energy is emitted by radionuclides in the form of packets of energy, photons. This discrete energy is characteristic of the emitting radionuclide and is the basic property for gamma-ray spectrometric research. By means of the intensity and energy level of gamma-ray photons, the source of the radiation can be determined (IAEA, 2003). In geological studies, gamma-ray spectrometry is often used to determine the relative abundances or concentrations of K, U and Th whose energy windows are centered, respectively, on 1.46, 1.76 and 2.61 MeVs, and also to determine the Total Concentration (TC) of the radioactivity with the sum of the windows of the whole spectrum (Adams and Gasparini, 1970; Minty, 1997; Wilford et al., 1997). One of the reasons why the elements K, U and Th are of interest in geological study is the half-life of these elements, compatible with the age of the Earth (Magill and Galy, 2005).

The field procedure in gamma-ray research depends on the purpose of the research. The sampling time will influence the accuracy of the measurement, the longer the sampling time, the more accurate it will be. The quality of the data also depends on the radioactivity of the source, the geometry of the survey, the volume, the efficiency and sensitivity of the detector. The consistency of the data measured along the outcrop must be such that the source-detector geometry is the same used in the spectrometer calibration (IAEA, 2003; 2010), an ideal condition that is not always reproduced in the field. The dimensions and shape of the sampled region are determined by the physical and chemical characteristics of the rock, such as density, porosity, fractures and mineralogical composition (Adams and Gasparini, 1970; IAEA, 2003).

Facies Analysis

The sedimentary facies were defined and analyzed in three outcrops (Figures 2b-d), where columnar sections (scale 1:10) were made for gamma-ray spectrometric profiling, as well as panoramic sections were produced for layer shape analysis. The interpretation of glacial

[1] **Nuclide** is the general term applied to all atomic forms of elements, comprising all isotopes of all elements. The nuclide is differentiated by its number and atomic mass and energy state (CNEN - Glossary of Terms Used in Nuclear Energy).

[2] **Gamma radiation** is the electromagnetic radiation emitted by an excited atomic nucleus during the process of passing to a lower state of excitation (Magill and Galy, 2005).

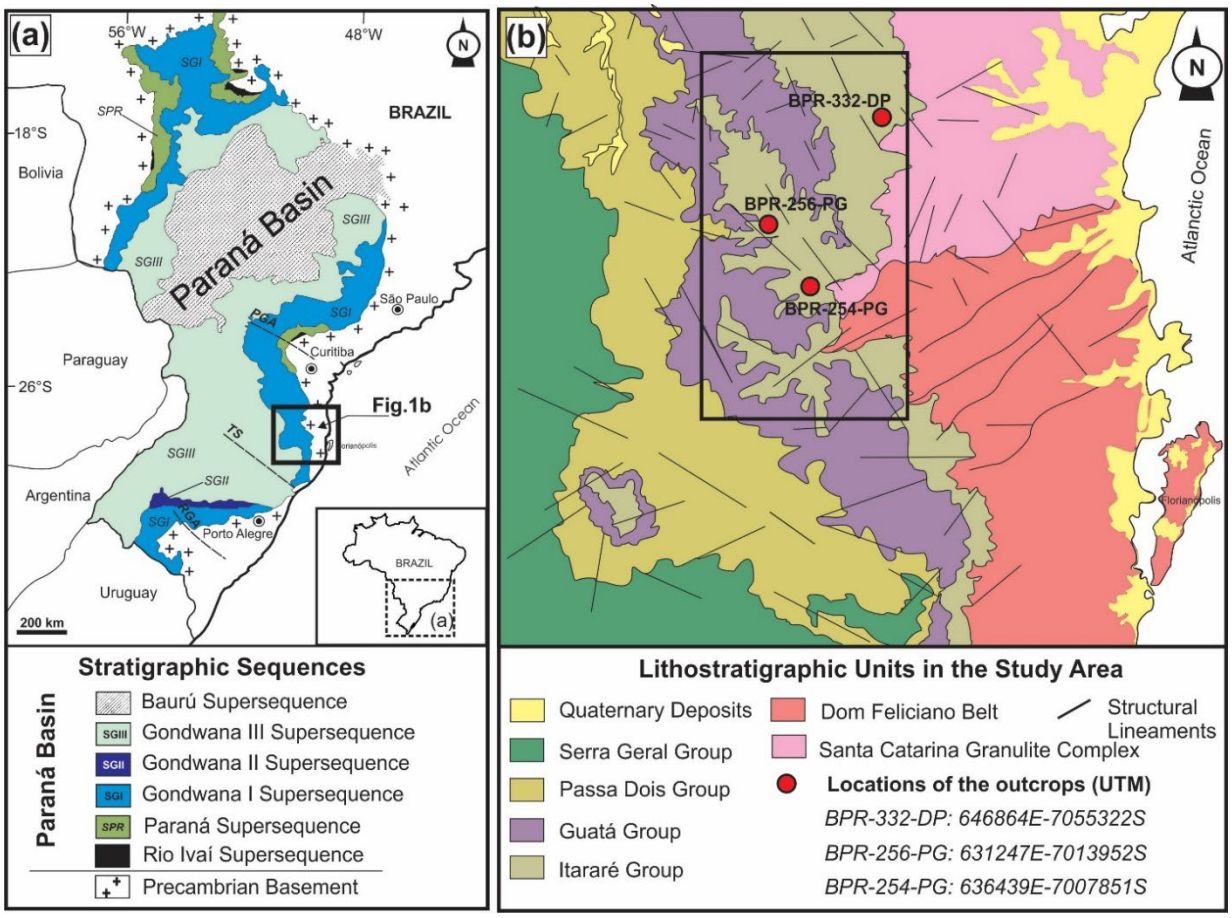

Figure 1: (a) Simplified geologic map of the Paraná Basin with the stratigraphic supersequences (after Milani, 2004); and (b) Close-up geological map of the Doutor Pedrinho and Presidente Getúlio regions with locations of the outcrops (from the Cartographic base of the Geological Survey of Brazil, 2014).

depositional environments was based on models by Rust (1977), Eyles et al. (1983), and Eyles and Eyles (2010). The interpretation of turbiditic systems was based especially on the models of Bouma (1962), Lowe (1982), Mutti (1992) and Haughton et al. (2009). The facies notation followed the methodology of Miall (1979).

Field Gamma-Ray Spectrometric Logging

The field GRS logging was supported by facies descriptions of three outcrops in *Doutor Pedrinho* and *Presidente Getúlio* regions (Figure 1a). The strata of these outcrops show broad lateral (> 30 m) and vertical (> 10 m) continuity, with well-preserved sedimentary structures and mineral composition. Seventy-five readings were performed on outcrop BPR-332-DP and 106 on outcrop BPR-256-PG from the Taciba Formation, and 94 readings on outcrop BPR-254-PG from the Campo Mourão Formation.

Potassium (%), uranium (ppm) and thorium (ppm) concentrations were obtained using a RS-330 portable gamma-ray spectrometer (Radiation Solutions Inc., Canada) of the Laboratório de Análise de Bacias Sedimentares e Reservatórios (LABAC - analysis laboratory of sedimentary basins and reservoirs) at Universidade Federal de Santa Catarina. This equipment has an energy resolution of 2.9 KeV/channel (1024 channels), practical resolution limit of the sodium iodide detector (Gilmore, 2008) that equips the instrument.

Samplings were carried out in outcrops that reproduced, as much as possible, the geometry used for equipment calibration. Samplings with a distance of less than 40 cm from the base and top of the outcrops were avoided to preserve measurements of counts unrelated to lithology due to the volume of detection of gamma radiation by the instrument. Readings were performed at regular spacing of 20 cm. This regularity in the acquisition allows for greater consistency in the description of variations in the radiometric profile associated with the stratigraphic one, allowing the identification of radiometric characteristics in response to lithological variations as well as the transition between depositional packages. The sampling time was 180 s, enough to keep the errors associated with the

concentration measurements below 10%. The average percentage errors associated with gamma-ray measurements, which will not be highlighted throughout the text, were between 1.5 and 3.0% for potassium, 2 and 5% for thorium and 7 and 9% for uranium (exceptionally 4% in the U1 - Depositional Unit 1). Errors associated with measurements are automatically calculated by the RS-330 internal algorithm.

Data were imported from the equipment using the RSAnalist software and then organized and processed in Python and Excel software. The gamma-ray spectrometric logs were associated with faciological and architectural data in columnar sections (1:10 scale). For data analysis and interpretation, tables and graphs were used to highlight patterns and features in sedimentary successions.

To validate the conversions performed in data treatment, the Dose Rate measured by the equipment (data imported and expressed in µRh-1 by the equipment) was compared with the Dose Rate calculated through the Total Count (ppm_eU) obtained through the concentrations of K, U and Th with sK/sU = 2.3 and sTh/sU = 0.44, according to IAEA (2003). The s_K/s_U ratio is the uranium equivalent of potassium, and the s_{Th}/s_U ratio is the uranium equivalent of thorium for a given instrument. The result had an average agreement of 99%, indicating that the count rate varies linearly with the gamma dose rate.

RESULTS AND DISCUSSIONS

Facies and Facies Associations

The Campo Mourão and Taciba formations, in the study area, present a wide variety of facies, composing an approximately 49 m thick succession (Figure 2a). Layers are tabular to lenticular, with gently undulating top and bottom, sometimes amalgamated. The main lithotypes include shale, fine- to medium-grained, occasionally coarse-grained sandstone. The facies associations are interpreted as glaciolacustrine environment characterized by tabular rhythmites (shale-siltite), black shales and thin-bedded turbidites (U1: Depositional Unit 1), and two submarine fans with thick-bedded turbidite systems (HDTf) and hybrid beds (debrites), which occur in the intermediate (U2a: Depositional Unit 2a) and in the upper (U2b: Depositional Unit 2b) portions of the succession (Figures 2b-d).

U1: Glaciolacustrine deposits with thin-bedded turbidite system

The U1 was recorded in outcrop BPR-254-PG (Figure 2b), which has lateral extension > 50 m and vertical extension > 19 m, comprising an agradational glaciolacustrine succession of tabular black shale, siltstone and very fine-grained sandstone. The main lithofacies identified in this outcrop includes Fl, Sm, Sh (Figures 3a-b), as well as Fm, Sr and Cc (Figure 2b). The Fl lithofacies is composed by black shale and gray siltstone with plane-parallel, sometimes undulated laminations and dispersed granules and pebbles of granite and gneiss (Ds). The lithofacies Sm/Ta, Sh/Tb and Sr/Tc occur intercalated with the lithofacies Fl/Te and Fm/Td. Some massive siltstone (Fm) and fine-grained sandstone (Sm) beds are cemented by carbonate (2 to 15 cm thick; Figure 2b). The Cc lithofacies include carbonate lenses with “cone-in-cone” structure.

The ‘Bouma’ sequence Ta, Tb, Tc, Td and Te in this outcrop indicates deposition from low-density turbidity flow (LDTf). Sandstone lenses (Sr/Tc) interbedded with siltstones and heterolithic facies indicate deposition by weak traction currents during the passage of dilute turbidity flows. Sections dominated by this type of deposition represent long periods of low sedimentation rate, punctuated by periods of deposition of diluted turbidites. A Bouma sequence is a set of sedimentary structures that form as result of the passage and deposition from turbidity currents in deep marine settings and the conceptual framework is widely applied to lacustrine environments (Shanmugam, 1997).

Paleocurrent data from sole marks and cross laminations indicate eastward sedimentary flows. Scoyenia-Mermia and Cruziana sp. ichnofacies were identified on the Te facies surface, which indicate a low-energy lacustrine continental environment. The soft-sediment deformation observed in this outcrop indicates deformation adjacent to glacier ice that exerts high-stresses on the sediment bodies by glacier ice.

U2: Submarine Fan Depositional System

The U2 includes two submarine fan depositional cycles and was recorded in the outcrops BPR-256-PG (U2a) and BPR-332-DP (U2b). Submarine fan depositional systems form the largest clastic accumulations in the deep sea and are considered a sediment-transfer system between the hinterland source area and the deep-sea environments.

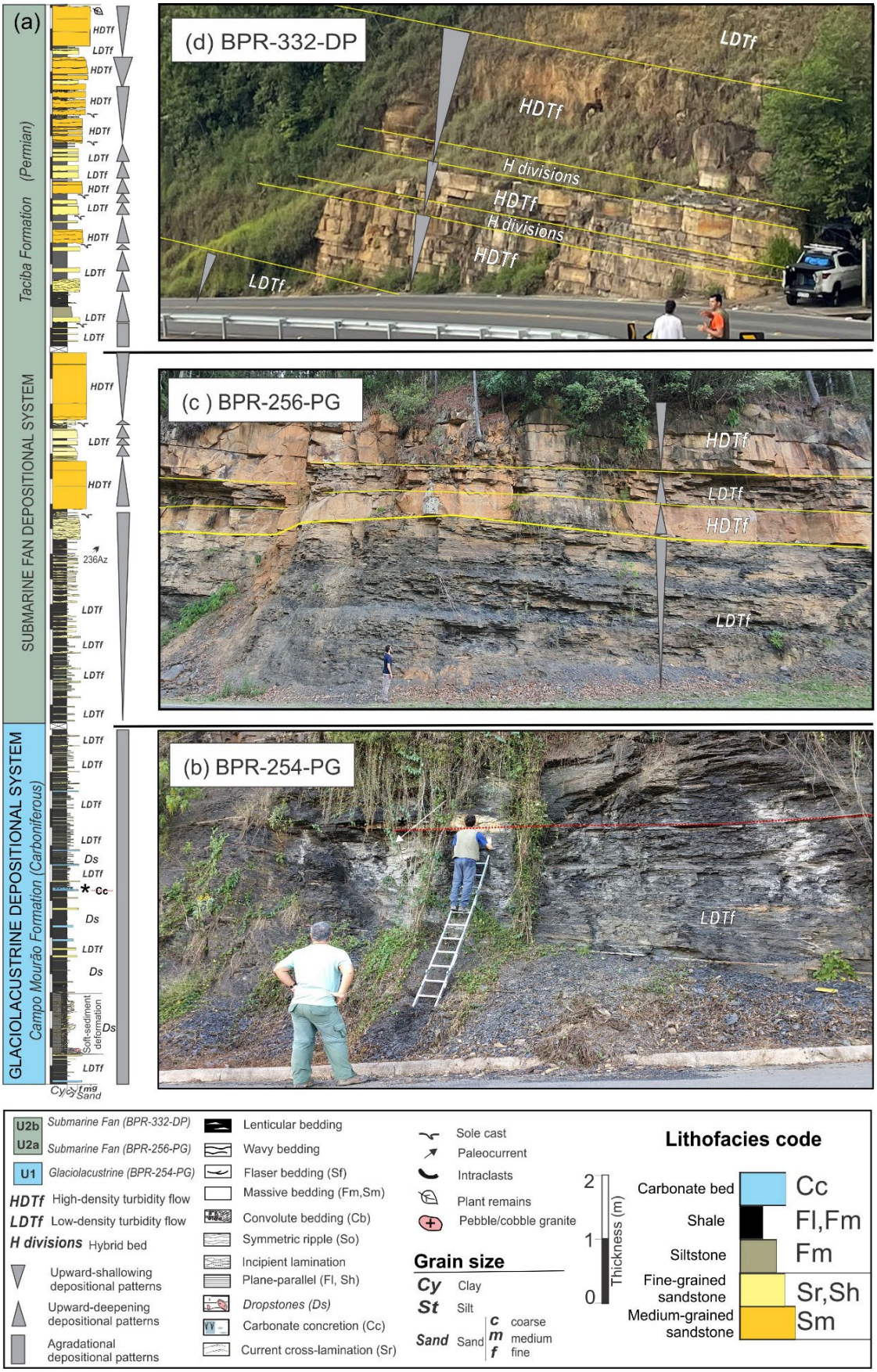

Figure 2: (a) Measured sections illustrating facies successions, grain size, sedimentary structures, and depositional system interpretations; (b-d) panoramic view of the outcrops BPR-254-PG, BPR-256-PG and BPR-332-DP.

The facies pattern in both submarine fans indicates deposition from high- to low-density turbidity flows (HDTf – LDTf) which have a high- to low-sediment concentration rates, respectively, whose main particle support mechanism is the turbulence (Mulder and Alexander, 2001).

The U2a (BPR-256-PG): comprises a progradational succession (from the base to the top; Figure 2c) of shales, siltstones, fine-grained sandstones, to thick tabular medium-grained sandstones, with load structure and scarce intraclasts of shale at the base. Intraclasts at the base of some sandstone indicate the passage from high-density turbidity flows (HDTf), which erode the semi-consolidated substrate (Td-e Bouma facies). Fine- to medium-grained sandstone (> 20 cm) presents massive (Sm/S3/F5), as well as plane-parallel (Sh/Tb/F7) or ripple cross-lamination (Sr/Tc/F6) structures. This facies association, including massive siltstone (Fm) or shale (Fl/Te), represents an important deposit of basin plain environments (Mutti, 1992) including channels which pass laterally to levee deposits, with incomplete Boume sequence (Figure 2d). The laminated sandstone (Sh/Tb/F7) is attributed to deposition from traction carpet flow.

The U2b (BPR-332-DP): comprises the facies Sm, Sr and Fl (Figures 3e-f), as well as Sh and Fm facies, which form tabular structures. The sandstones are medium-grained, moderately selected, normally graded, with a massive structure (Sm/S3/F5), with intraclasts of shale and turboglyphs at the base. These channels develop erosional features (Figure 3f) and indicate deposition unidirectional flow, being of great importance in understanding the flow conditions, which record the deposition of a relatively dilute suspension with low rates of sediment precipitation (Talling et al., 2012). In long-time hyperpycnal flows, they are associated with massive sandstones (Sm/S3) and laminated (Sr/Sh/F6) sandstones where thick amalgamated packages occur with alternation of these facies, caused by momentary changes in flow conditions (Zavala and Pan, 2018). The distal lobes comprise thick-heterolithic successions with massive sandstone at the base (Sm/S3), plane-parallel lamination (Sh/F6) or current cross-lamination (Sr/F6), followed by siltstone or shale (Fl/Td-e)

This submarine fan includes debrite deposits (hybrid deposits) that contain four divisions (Haughton et al., 2009; see Figure 3f). The H1 division results from a high-density turbidity current (like S3 Lowe facies). The H2 division includes clean and clay-rich sandstones, with sheared dewatering pipes that result from episodic near-bed turbulence damping, in a flow transitional between turbidity current and debris flow. This division is overlain by clean sandstones with parallel and ripple cross-lamination that result from low-density turbidity current. Finally, this division is capped by laminated shales (H5 division) that result from suspension.

Stratigraphic Distribution of Gamma Radiation Data

The K, eU and eTh concentrations in outcrops reveal distinct stratigraphic patterns (Figures 4b-c; Table 1). The depositional units can be discriminated by means of total gamma counts (TC), contents and spectrometric concentrations. U1 has $TC_{mean} > 28$ ppm_eU, U2a has 14 ppm_eU $\leq TC_{mean} \leq 28$ ppm_eU, and U2b has $TC_{mean} <$ 14 ppm_eU (Figure 5a). In the K-eU-eTh diagram, the U1 is discriminated from the U2b by the higher uranium content in the U1 and the higher potassium content in the U2b (Figure 5b). The thorium contents of the U2b are, on average, lower than those of the U2a. In terms of spectrometric concentration (Figures 5c and 5d), the U1 has concentrations of $K \geq 3.5$ %, $Th \geq 20$ ppm and $U \geq 5.7$ ppm; the U2b has concentrations of $K < 3.5$ %, $eTh < 20$ ppm and $eU < 5.7$ ppm. In the U2a the concentrations are distributed over the entire range. In its lower strata the concentrations tend to those of the U1, and in its upper strata they tend to those of the U2b.

The U1, which is mainly characterized by glaciolacustrine thin-laminated rhythmites as well as thin-bedded turbidites, is the unit with the highest average concentrations of potassium, thorium and uranium, $TC_{mean} = 29.8$ ppm_eU. The layers between 8.6 m and 12.9 m record the highest concentrations of gamma rays, $TC_{mean} = 34.3$ ppm_eU, with contributions mainly from uranium and thorium. This stratigraphic interval is intercalated by a layer (~ 20 cm thick) of fine-grained carbonate sandstone of great lateral extension that stands out in the gamma radiation logs due to the decrease in the concentration of radionuclides. Also noteworthy is the stratigraphic interval between 2.1 m and 5.7 m, with the lowest concentrations of K, eTh and eU ($TC_{mean} = 24.8$ ppm_eU). This decrease in gamma radiation is, probably, due to the increase in carbonate cement in sandstones in these strata. Similar decreases in concentrations are recorded in other laminae and thin layers of carbonates, which are highlighted in Figure 4b. The sparse dropstones present in the basal part of the unit, which attest to the glacial influence in retreat, are not significant to influence the measurements of radionuclide concentrations.

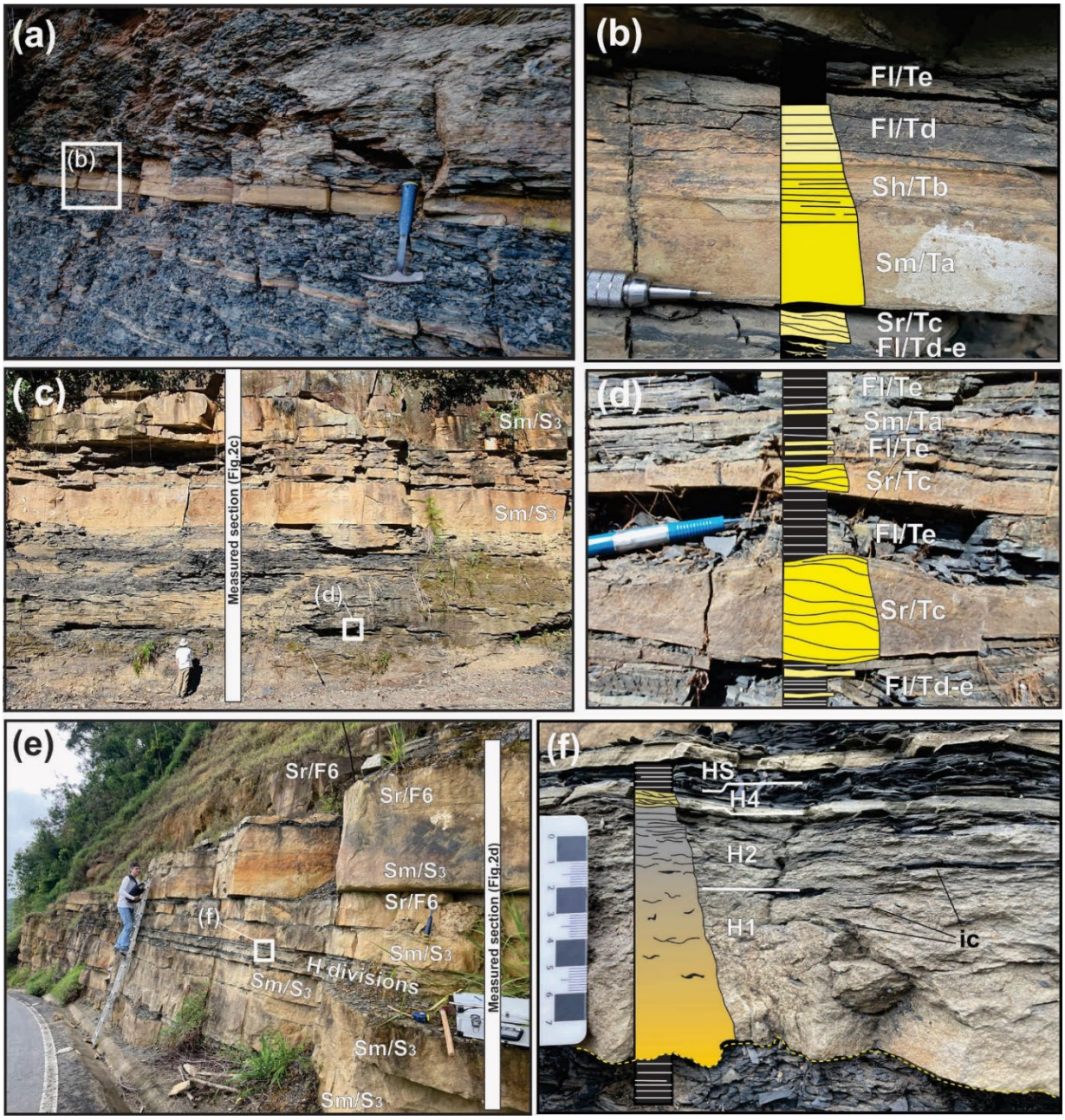

Figure 3: Sedimentary facies succession exposed in the outcrops: (a-b: BPR-254-PG) rhytimite, black shale and thin-bedded turbidites (Sequence of Bouma); (c-d: BPR-256-PG) thick and thin-bedded turbidite architecture (channel and levees with Lowe sequence, 1982); (e: BPR-332-DP) thick-bedded turbidite facies (with Lowe, 1982, and Mutti, 1992, facies); and (f: BPR-332-DP) hybrid bed with H divisions of Haughton et al. (2009).

The U2a has a higher concentration of gamma rays in its lower strata than in its upper strata (Figure 4b). The lower strata (0 m to 7 m) are composed of shales and rhythmites (silty claystones and silty sandstones) intercalated with laminae of fine-grained sandstones. These facies are similar to the facies of the U1 to which they overlap, and it is difficult to differentiate them with assurance in the field work. The distinction of these strata is perceptible through TC; however, it is through the uranium content that greater confidence is obtained in the individualization of these strata. The uranium content in the lower strata of the U2a is significantly lower than its content in the U1. The ratio of the average uranium concentration of the lower section of the U2a to the average uranium concentration of the U1 is 58%. The distinction between these units is also immediate when comparing eTh/eU and eU/K ratios or concentration graphs (Figure 4c). Likewise, the higher content of potassium and thorium in relation to uranium discriminates these pelitic strata of the U2a from its top,

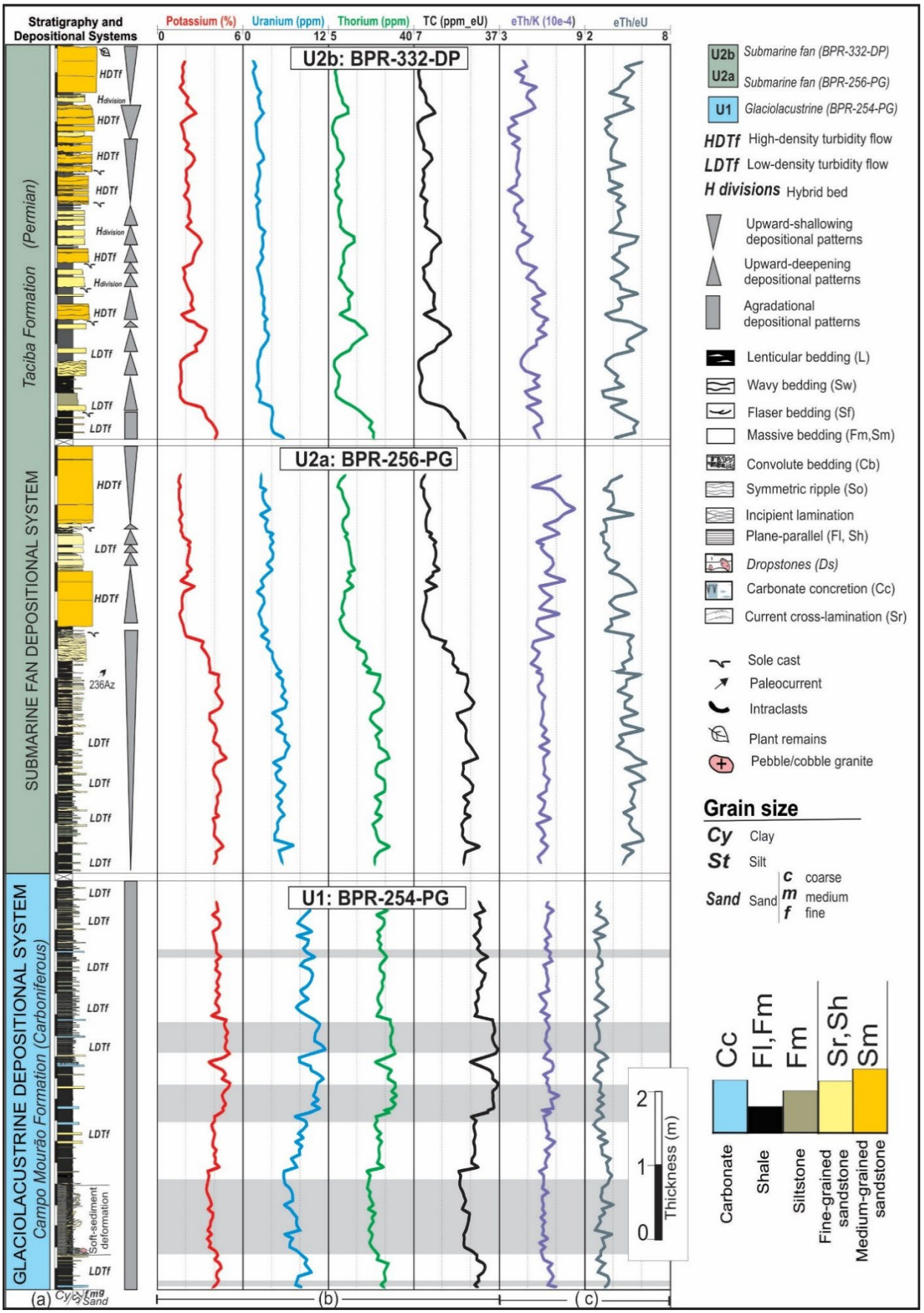

Figure 4: (a) Lithostratigraphic successions, (b) gamma-ray spectrometric logs and (c) radionuclide ratios of the studied depositional units (see locations of the outcrops in Figure 1).

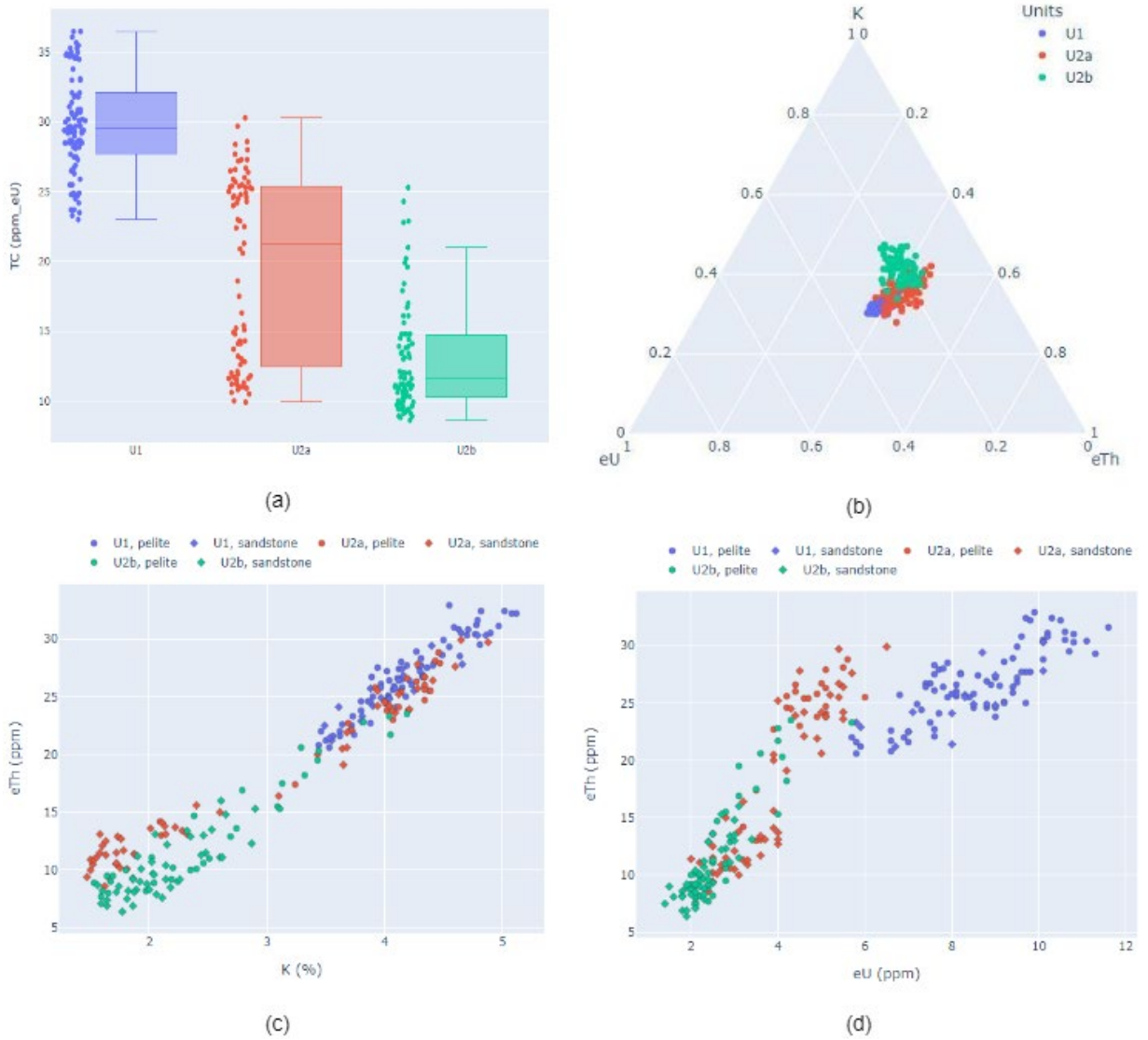

Figure 5: Division of depositional units by (a) Total Count, (b) diagram K-eU-eTh, (c) eTh x K and (d) eTh x eU.

where sandstones predominate. This is best perceived by the values of the eTh/eU and eU/K ratios, higher and lower, respectively, in relation to the top of the unit (Table 1). There are, therefore, decreasing values for the eTh/eU ratio and increasing for the eU/K ratio in the sequence: (i) 'common' shale and pelitic facies, (ii) sandstone facies and (iii) black shale.

The intermediate strata of the U2a are constituted by sandstones gradually replacing the pelites that predominate in the lower section. They represent prograding lithofacies with increasing sediment input in relation to the lower section. This transition section between the high and low concentrations of the U2a shows a funnel-shaped pattern (ascending decrease in radioactivity) evidenced by the increase in grain size, an indication of the increase in depositional energy levels. There is also a relative approximation between the concentrations of thorium and potassium, indicating hydrodynamic changes, faster transport, with less time of exposure to weathering, or perhaps diagenetic enrichment of potassium. The study of petrographic thin section may help to answer this question.

The upper strata of the U2a, which comprise lobes, channels and levees, have the lowest gamma radiation values. They are characterized by the predominance of fine to medium sandstone with laminae and centimetric layers of intercalated pelites. In this section, there is a slow and gradual decrease in the concentrations of thorium, potassium and uranium, accompanied by oscillations, mainly of uranium.

The U2b is predominantly fine- to coarse-grained sandstone with thick layers (decimetric to metric) often

amalgamated, sometimes with erosive bases and intercalated shales. This unit has the lowest concentrations of potassium, thorium and uranium sampled in this work (Table 1). The TC_{mean} of this unit is equivalent to 44% of the TC_{mean} of the U1, which has the highest concentrations. The largest gamma-ray records from this unit, with decreasing values towards the top, occur at the base of this unit, a layer of laminated pelites with a thickness of 1.2 m.

Correlations between outcrops (and wells) considering only the TC and facies description can lead to misunder. For example, there are similarities between the TC of the U1 sections with sections of the U2a and U2b. However, when considering the concentrations, or contents, of K, eU and eTh and their ratios, distinct characteristics are observed between these units. While in the U1 the contents of K, eU and eTh in relation to TC are 0.32, 0.29 and 0.39 respectively, in the U2a they are 0.36, 0.21 and 0.42, and in the U2b they are 0.41, 0.20 and 0.39. That is, the contributions of radioelements to TC in the U1 are comparable to each other due to uranium enrichment. In contrast, even with lower concentrations of potassium in the U2a and U2b units, its content is practically twice the uranium content and, therefore, correlating sections of these units through the TC leads to interpretation errors.

Gamma-Ray Spectrometry and Grain Size

The source rock is the main factor that controls the mineralogy of siliciclastic sedimentary particles that are transported into a basin. However, depending on the climatic regime, weathering promotes the breakdown and decomposition of the rock, generating two phases, one soluble and one residual. Each of these phases contributes in a different way to the formation of sedimentary rocks, either with the precipitation of the soluble phase in a sedimentation environment or with the supply of residual detrital grains to the depositional basins. On the other hand, during transport, the sediments undergo differential abrasion according to the physical resistance of each mineral. So, hydrodynamic selection during sediment transport changes mineral abundances and proportions as a function of their densities and shapes (Remus et al., 2008).

Gamma radiation levels result from mineralogy and not grain size; however, as mentioned above, changes in grain size are accompanied by changes in mineralogy (Myers and Bristow, 1989) and manifest in gamma radiation readings. The sensitivity of the gamma-ray spectrometer to sandstone and pelitic facies, that is, the ability to discriminate these facies, is dependent on their mineralogical (and chemical) compositions and, above all, on the lithostratigraphic distribution of the sedimentary layers.

The pelites from the U1 attest deposition from low energy, associated with thin-bedded turbidites. The predominance of pelites over laminae and thin layers of sandstone in these environments tends to homogenize the gamma radiation readings between these lithotypes. In the depositional units U2a and U2b, TC and concentrations of potassium, thorium, uranium decrease upwards, and reflect the increase in grain size towards the top, according to the stratigraphic profile, which passes from predominantly pelitic to sandy strata (Figures 4a and 4b). The overlapping of the concentration values is visually noted in Figure 6. The best sensitivity is evidenced in the U2a by the potassium and thorium contents, whose minimum values in the pelites are above the median of the sandstones (Figures 6b and 6c). Uranium is the least sensitive to lithologies in all units; this is associated with its irregular distribution in depositional environments due to its great mobility in weathering and diagenesis processes (Figure 6d).

Although the distinction between lithofacies in the studied units is not assured by means of TC or gamma-ray spectrometry, the distinction between pelitic-rich strata from sandy-rich strata of the U2a is well highlighted in the gamma-ray spectrometric record (Figure 4b).

In the U2a and U2b units, the thorium and potassium content in relation to the uranium content discriminates pelite from sandstones. The high eTh/eU ratios (Figure 4c) and low eU/K ratios evidence the concentration of pelite. This result is therefore in accordance with the usage of the CGR (Clay Gamma-Ray; Th + K) instead of the GRS (Gamma-Ray Spectrometry; Th + K + U) as a parameter to estimate the volume of clay (Rider, 1996; Ellis and Singer, 2008).

Gamma-Ray Spectrometry, Sedimentary Processes and Environments

Through the eTh/K ratio and the concentrations of eTh and K in a sedimentary sequence, it is possible to access a set of information about the sedimentation process, intensity of chemical weathering and homogeneity of provenance (Basu et al., 2009).

Table 1: Mean and standard deviation (std) of radioelement concentrations and ratios.

Unit	Number of Samples		K (%)		eU (ppm)		eTh (ppm)		eTh/K (10^{-4})		eTh/eU		eU/K (10^{-4})		TC (ppm_eU)	
			mean	std	mean	std	mean	std	mean	std	mean	std	mean	std	mean	std
U1	sand	16	4.07	0.44	8.2	1.4	25.4	3.0	6.2	0.2	3.2	0.4	2.0	0.2	28.7	3.6
	pelite	78	4.21	0.41	8.6	1.4	26.7	3.1	6.3	0.3	3.1	0.3	2.0	0.2	30.1	3.5
	total	94	4.18	0.42	8.5	1.4	26.5	3.1	6.3	0.3	3.1	0.3	2.0	0.2	29.8	3.5
U2a	sand	61	2.86	1.17	3.9	1.2	17.5	6.6	6.3	0.6	4.5	0.9	1.5	0.3	18.2	6.6
	pelite	45	4.30	0.74	5.7	1.9	26.1	4.8	6.1	0.3	4.8	0.9	1.3	0.3	27.1	5.4
	total	106	3.48	1.23	4.7	1.8	21.2	7.2	6.2	0.5	4.6	0.9	1.4	0.3	22.1	7.5
U2b	sand	42	2.10	0.35	2.3	0.5	10.1	2.5	4.7	0.7	4.4	0.6	1.1	0.2	11.6	2.2
	pelite	33	2.58	0.80	2.9	0.9	13.5	5.2	5.2	0.7	4.6	0.8	1.1	0.2	14.8	4.9
	total	75	2.31	0.63	2.6	0.7	11.6	4.2	4.9	0.7	4.5	0.7	1.1	0.2	13.0	3.9

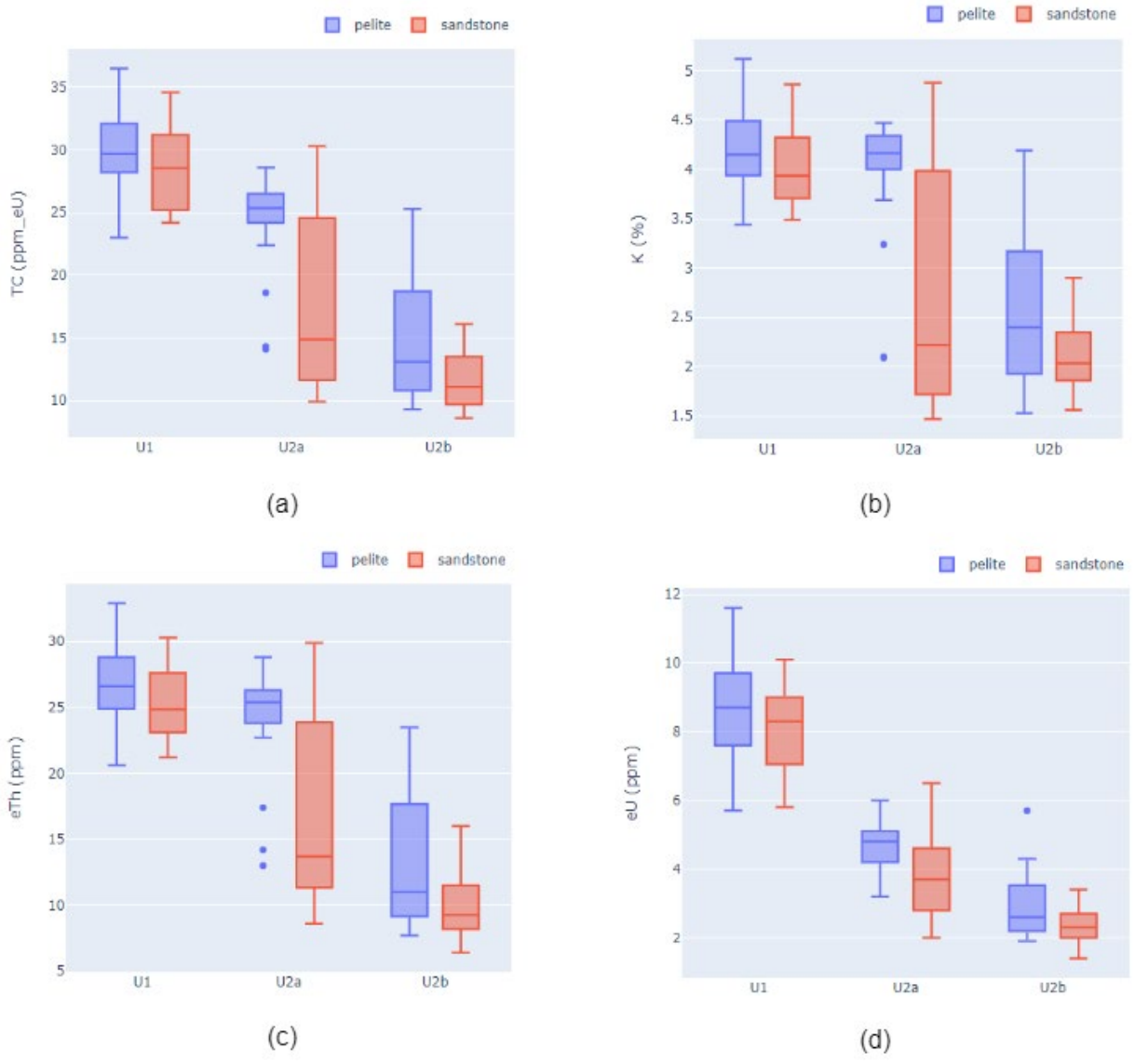

Figure 6: Concentration of radioelements per unit and grain size. (a) TC, (b) Potassium, (c) equivalent Thorium and (d) equivalent Uranium.

In the U1, the trendline of the eTh/K ratio is practically constant, with a small increase towards the top. The eTh/K ratio, within the margin of error, was between 6 and 7 throughout the interval (Figure 4c). For simplification, it is assumed that thorium in a depositional environment has a detrital nature and is chemically inert (Bessa, 1995). As, in this unit, variations in thorium concentration are accompanied by variations in potassium concentration (correlation factor r = 0.94), it can be assumed that the conditions of the deposition period remained relatively constant, at least without alteration of the minerals responsible for hosting potassium; except, by hypothesis, for the greater or lesser sediment input, evidenced by the fluctuation of the thorium and potassium concentration. Also, according to Bessa (1995), the concentration of a highly soluble element coupled to the concentration of a highly insoluble element may indicate that the concentrations of these elements in the sediments were the result of a primary deposition process, and not of diagenetic reactions.

In the U2a, the eTh/K ratio increases towards the top, indicating a greater water depth and distance from the shoreline (Myers and Wignall, 1987) at the bottom of this unit. Changes in thorium concentrations are accompanied by changes in potassium throughout the unit, maintaining a high correlation. In the lower and intermediate strata, the eTh/K ratio remains practically constant, suggesting a common provenance for the sediments of these strata. In the upper strata of this unit, dominated by sandstones, the average eTh/K ratio is 6.6. According to Basu et al. (2009), sandstones with eTh/K > 6 indicate intense chemical weathering; however, this is not the deposition condition of this unit, which is in a stage of glacial advance. Glacial and proglacial sediments, which predominate in the study area, are dominated by mechanical rather than chemical processes (Goldschmidt, 1954 *apud* McLennan, 2001). The proximal lobes, channels and levees show large fluctuations in the eTh/K ratio, conditioned by fluctuations in thorium concentration. This may indicate oscillations in mechanical energy, changing hydrodynamic conditions during deposition. The increase in the sandstone/pelite ratio towards the top of this depositional unit, evidenced by the thickening of the sandstone layers, characterizes the progradation of the submarine fan.

Just as sedimentary processes can be evidenced by the eTh/K ratio, the eTh/eU ratio is frequently used to estimate the redox conditions of the depositional environment (Doveton, 1991) and the characterization of these environments (Adams and Weaver, 1958 *apud* Basu et al., 2009). Low eTh/eU ratio due to high uranium concentration may be associated with marine condensed sequences and may indicate an environment that acted to fix uranium under the influence of reducing conditions (Myers and Wignall, 1987). On the other hand, high eTh/eU ratio indicates the mobilization of uranium due to weathering in an oxidizing environment, with the influence of oxygen availability, presence of water and organic materials, or even, the deposition of heavy minerals rich in thorium (Basu et al., 2009).

The mean value of the eTh/eU ratio (Table 1) of the U1, the lowest compared to the other units, associated with the high concentration of uranium, indicates that this unit is inserted in the most reducing environment among those sampled. The high concentration of uranium is mainly responsible for the distinction of this unit. This higher uranium content may be the result of enrichment in authigenic U that tends to be precipitated under anoxic conditions (Lüning and Kolonic, 2003). Since the measured uranium is the sum of detrital uranium and authigenic uranium, an estimate of the fraction of authigenic uranium can be obtained (Myers and Wignall, 1987), considering that the eTh/eU ratio in non-reducing environments is due to detrital elements.

By means of Equation (1) and taking as reference the average value of the eTh/eU ratio = 5.0 (from pelites of the U2a and U2b, supposedly non-reducing), an average concentration of 3.2 ppm was obtained for authigenic uranium and 5.3 ppm for detrital uranium:

$$eU_{measured} = U_{detrital} + U_{authigenic} \quad (1)$$

where:

$$U_{detrital} = Th_{detrital}/5 \text{ and } Th_{detrital} = eTh_{measured.} \quad (2)$$

The mean ratio of estimated authigenic uranium to measured uranium, considering the entire unit, is 37 %. The highest mean ratio, 40 %, was obtained from 7.3 m upwards and possibly corresponds to the most intense period of anoxia. This ratio was not affected by the highest concentrations of the three radioelements in the strata between 8.6 m and 12.9 m. However, in the strata between 2.1 m and 5.7 m, this ratio is only 33 % and corresponds to the region of lower uranium concentration (in absolute and relative values; in this interval the eTh/eU ratio increases from 3.0 to 3.3).

In the shales and thin turbidites of the lower strata of the U2a, the average eTh/eU ratio (~ 5.0) indicates a lacustrine environment or a shallow marine environment. According to Adams and Weaver (1958, *apud* Basu et al., 2009), most marine sediments have eTh/eU ratios between 3 and 5. However, North and Boering (1999) verified that continental sediments can also present these values for the eTh/eU ratio. The intermediate strata of the U2a show oscillations and the decrease in this ratio toward the top of the unit (predominantly sandstone) due to the decrease of eTh in relation to eU. The average of this ratio in the U2a is 4.6, indicating neither a reducing nor a strongly oxidizing environment, and remains stable in the U2b, with an average value of 4.4.

CONCLUSIONS

Facies association distribution in the Presidente Getúlio and Doutor Pedrinho regions documents a glaciolacustre environment to Campo Mourão Formation and two submarine fans to Taciba Formation. The internal architecture of these sedimentary successions was compared with facies models and also used to infer flow processes in these sedimentary environments. Linked debrites attest transformation from turbulent to laminar flow. Mud clasts in clean sandstones suggest that flow transformation may be aided by disaggregation of mud clasts within the flow.

The spectral gamma-ray record proved to be effective method for the delimitation of depositional sedimentary units of the Itararé Group.

The relationship between radiometric data and grain size indicated that, in field work, lithostratigraphic distribution (the lithological variation between sedimentary layers) has a great influence on the gamma-ray spectrometer ability to distinguish lithotypes. The spectrometric data proved to be useful to differ shales. High uranium concentration characterizes the Lontras Member black shales and distinguishes them from 'common' shales from the Taciba Formation. In general, for the studied outcrops, decreasing values of the Th/U ratio establish the following sequence: (i) 'common' shale and pelitic facies, (ii) sandstone facies and (iii) black shale.

The applicability of gamma-ray spectrometry associated only with the description of facies for the interpretation of sedimentary processes and environments is limited to some assumptions at particular intervals. For example: (i) the relative stability in sedimentation conditions given by the strongly positive correlation between potassium and thorium; (ii) variations in sediment input given by changes in concentrations without changing their ratios; (iii) provenance homogeneity as a function of Th/K ratio stability; (iv) the identification of progradation indicated by the increase of the Th/K ratio; (v) variations in hydrodynamic conditions as a function of thorium oscillations; (vi) the distinction between reducing and non-reducing environments by the low Th/U ratio associated with high uranium concentrations.

ACKNOWLEDGMENTS

To PETROBRAS (Petróleo Brasileiro S.A.), which, through financial support to the project "Machine Learning Techniques for Recognition of Sedimentological Patterns of Turbiditic Systems", made the field research possible. To Universidade Federal de Santa Catarina (UFSC), Laboratório de Análise de Bacias Sedimentares e Reservatórios (LABAC) and Grupo de Análise de Bacias e Reservatórios (ANBA) for the support and infrastructure, and to the colleagues and professors who collaborated with the work activities of field.

REFERENCES

Adams, J.A.S., and P. Gasparini, 1970, Gamma-Ray Spectrometry of Rocks. Series Methods in Geochemistry and Geophysics: Elsevier Publishing Company, Netherlands, 308 pp.

Anjos, R.M., Veiga, R., Carvalho, C., Macario, K.D., and P.R.S. Gomes, 2007, Geological provenance of Quaternary deposits from the southeastern Brazilian coast: Nuclear Physics A, Netherlands, **787**, 642–647, doi: 10.1016/j.nuclphysa.2006.12.075.

Basu, H., K.M., Kumar, S. Paneerselvam, and A. Chaki, 2009, Study of provenance characteristics and depositional history on the basis of U, Th and K abundances in the Gulcheru Formation, Cuddapah Basin in Tummalapalle-Somalollapalle areas, Cuddapah-Anantapur districts, Andhra Pradesh: Journal of the Geological Society of India, **74**, 318–328, doi: 10.1007/s12594-009-0136-3.

Bessa, J.L., 1995, High-Resolution Outcrop Gamma-Ray Spectrometry of the Lower Lias, Southern Britain: PhD Thesis, Saint Edmund Hall and Dept. of Earth Sciences, Oxford. 212 pp.

Bouma, A.H., 1962, Sedimentology of some flysch deposits: a graphic approach to facies interpretation: Elsevier, Amsterdam, 168 pp.

Buso, V.V., C.D. Aquino, P.S.G. Paim, P.A. De Souza, A.L. Mori, C. Fallgatter, J.P. Milana, and B. Kneller, 2019, Late Palaeozoic glacial cycles and subcycles in western Gondwana: Correlation of surface and subsurface data of the Paraná Basin, Brazil: Palaeogeography, Palaeoclimatology, Palaeoecology, **531**, B, 1–16, doi: 10.1016/j.palaeo.2017.09.004.

Castro, M.R. De, J.A.J. Perinotto, and J.C. de. Castro, 1999, Fácies, análise estratigráfica e evolução pós-glacial do Membro Triunfo/Formação Rio Bonito, na faixa subaflorante do norte catarinense: Revista Brasileira de Geociências, **29**, 4, 533–538, doi: 10.25249/0375-7536.1999294533538.

Costa, H.S., M.S. Nascimento, and F.J.F. Ferreira, 2018, Clay minerals and gamma-ray spectrometry as paleoclimatic indicators in the Gondwana's sedimentary sequences, Santa Catarina, Brazil: Revista Brasileira de Geofísica, **36**, 3, 345-359, doi: 10.22564/rbgf.v36i3.1954.

Davies, S.J., and T. Elliott, 1996, Spectral gamma ray characterization of high resolution sequence stratigraphy: examples from Upper Carboniferous fluvio-deltaic systems, County Clare, Ireland: Geological Society of London, Special Publications, **104**, 25-35, doi: 10.1144/GSL.SP.1996.104.01.03.

D'avila, R.S.F., 2009, Sequências Deposicionais do Grupo Itararé (Carbonífero e Eopermiano), Bacia do Paraná, na Área de Dr. Pedrinho e Cercanias, Santa Catarina, Brasil: Thesis, Universidade do Vale do Rio dos Sinos – UNISINOS, RS, Brazil, 192 pp.

Doveton, J.H., 1991, Lithofacies and geochemical facies profiles from nuclear wireline logs: New subsurface templates for sedimentary modeling, *in* Franseen, E.K., W.L. Watney, C.J. Kendall, and W. Ross, Eds., Sedimentary modelling-computer simulations and methods for improved parameter definition: Kansas Geological Survey Bulletin, **233**, 101–110.

Ellis, D.V., and J.M. Singer, 2008, Well Logging for Earth Scientists: 2nd ed., Springer, Netherlands, 692 pp, doi: 10.1007/978-1-4020-4602-5.

Eyles, N., C.H. Eyles, and A.D. Miall, 1983, Lithofacies types and vertical profile models; an alternative approach to the description and environmental interpretation of glacial diamict and diamictite sequences: Sedimentology, **30**, 393–410, doi: 10.1111/j.1365-3091.1983.tb00679.x.

Eyles, C. H., and N. Eyles, 2010, Glacial Deposits, *in* James, N.P., and R.W. Dalrymple, Eds., Facies Models: 4. ed., Toronto: Geotext, 73–106.

França, A.B., and P.E. Potter, 1988, Estratigrafia, ambiente deposicional e análise de reservatório do Grupo Itararé (Permocarbonífero), Bacia do Paraná (Parte 1): Boletim de Geociências da Petrobras, **2**, 147–191.

Gilmore, G.R., 2008, Practical Gamma-ray Spectrometry: 2nd ed., John Wiley & Sons Ltd., United Kingdom, 387 pp, doi: 10.1002/9780470861981.

Gould, K.M., D.J.W. Piper, G. Pe-Piper, and R.A. Macrae, 2014, Facies, provenance and paleoclimate interpretation using spectral gamma logs: Application to the Lower Cretaceous of the Scotian Basin: Marine and Petroleum Geology, **57**, 445–454, doi: 10.1016/j.marpetgeo.2014.06.008.

Haughton, P.D.W., C.E. Davis, W.D. Mccaffrey, and S. Barker, 2009, Hybrid sediment gravity flow deposits – Classification, origin and significance: Marine and Petroleum Geology, **26**, 1900–1918, doi: 10.1016/j.marpetgeo.2009.02.012.

IAEA - International Atomic Energy Agency, 2003, Guidelines for Radioelement Mapping Using Gamma Ray Spectrometry Data: IAEA-TECDOC-1363: International Atomic Energy Agency, Austria, 184 pp.

IAEA - International Atomic Energy Agency, 2010, Radioelement Mapping: IAEA Nuclear Energy Series – nº NF-T-1.3, Austria, 108 pp.

Lowe, D.R., 1982, Sediment Gravity Flows: II.: depositional models with special reference to the deposits of high-density turbidity currents: Journal of Sedimentary Petrology, **1**, 52, 279–297, doi: 10.1306/212F7F31-2B24-11D7-8648000102C1865D.

Lüning, S., and S. Kolonic, 2003, Uranium spectral gamma-ray response as a proxy for organic richness in black shales: applicability and limitations: Journal of Petroleum Geology, **26**, 2, 153–174, doi: 10.1111/j.1747-5457.2003.tb00023.x.

Magill, J., and J. Galy, 2005, Radioactivity Radionuclides Radiation: Springer, Germany, 259 pp.

Mclennan, S. M., 2001, Relationships between the trace element composition of sedimentary rocks and upper continental crust: Geochem. Geophys. Geosyst., **2**, 4, 1021, doi: 10.1029/2000GC000109.

Menezes, M.T.F., and M.S. Nascimento, 2015, Petrografia e Diagênse de Arenitos Permianos da Bacia do Paraná, Região de Alfredo Wagner, Santa Catarina: Anais do IX Simpósio Sulbrasileiro de Geologia, Florianópolis, SC, Brazil.

Miall, A.D., 1979, Mesozoic and Tertiary geology of Banks Island, Arctic Canada, the history of an unstable craton margin: Geol. Survey of Canada, Memoir 387, 235 pp, doi: 10.4095/105620.

Milani, E.J., 2004, Comentários sobre a origem e a evolução tectônica da Bacia do Paraná, *in* Mantesso-Neto V., A. Bartorelli, C.D.R. Carneiro, and B.B. Brito Neves, Eds., Geologia do Continente Sul-Americano: Beca, Brazil, 265–280 pp.

Minty, B.R.S., 1997, Fundamentals of Airborne Gamma-ray Spectrometry: Journal of Australian Geology & Geophysics, **17**, 2, 39–50.

Mulder, T., and J. Alexander, 2001, The physical character of subaqueous sedimentary density flows and their deposits: Sedimentology, **48**, 269–299, doi: 10.1046/j.1365-3091.2001.00360.x.

Mutti, E., 1992, Turbidite Sandstones: Agip and Università di Parma, Italy, 275 pp.

Myers, K.J., and P.B. Wignall, 1987, Understanding Jurassic Organic-rich Mudrocks — New Concepts using Gamma-ray Spectrometry and Palaeoecology: Examples from the Kimmeridge Clay of Dorset and the Jet Rock of Yorkshire, *in* Leggett, J.K., and G.G. Zuffa, eds., Marine Clastic Sedimentology: Springer, Netherlands, 172–189, doi: 10.1007/978-94-009-3241-8_9.

Myers, K.J., and C.S. Bristow, 1989, Detailed sedimentology and gamma-ray log characteristics of a Namurian deltaic succession II: gamma-ray logging, *in* Whateley, M.K.G. and K.T. Pickering, eds., Deltas: sites and traps for fossil fuels: Geological Society of London, Special Publication, **41**, 81–88, doi: 10.1144/GSL.SP.1989.041.01.07.

Neves, L.F., C.C.F. Guedes, and F.F. Vesely, 2019, Facies, petrophysical and geochemical properties of gravity-flow deposits in reservoir analogs from the Itararé Group (late Carboniferous), Paraná Basin, Brazil: Marine and Petroleum Geology, **110**, 717–736, doi: 10.1016/j.marpetgeo.2019.07.038.

Noll, S.H., and R.G. Netto, 2018, Microbially induced sedimentary structures in late Pennsylvanian glacial settings: A case study from the Gondwana Paraná Basin: Journal of South American Earth Sciences, **88**, 385–398, doi: 10.1016/j.jsames.2018.09.010.

North, C.P., and M. Boering, 1999, Spectral gamma-ray logging for facies discrimination in mixed fluvial-eolian successions: A cautionary tale: American Association of Petroleum Geologists, AAPG Bulletin, United States, **83**, 1, 155–169, doi: 10.1306/00AA9A2A-1730-11D7-8645000102C1865D.

Remus, M.V.D, R.S. Souza, J.A. Cupertino, L.F. De Ros, N. Dani, and M.L. Vignol-Lelarge, 2008, Proveniência sedimentar: métodos e técnicas analíticas aplicadas: Revista Brasileira de Geociências, **38**, 2-Suppl., 166–185, doi: 10.25249/0375-7536.2008382S166185.

Rider, M.H., 1996, The geological interpretation of well logs: 2nd ed., Whittles Publishing, Scotland, 280 pp.

Rust, B.R., 1977, Mass flow deposits in a Quaternary succession near Ottawa, Canada: diagnostic criteria for subaqueous outwash: Can. J. Earth Sci., **14**, 3, 175–184, doi: 10.1139/e77-020.

Schneider, R.L., H. Mühlmann, E. Tommasi, R.A. Medeiros, R.F. Daemon, and A.A. Nogueira, 1974, Revisão estratigráfica da Bacia do Paraná: 28 Congresso Brasileiro de Geologia, Sociedade Brasileira de Geologia, Porto Alegre, RS, Brazil, **1**, 41–65.

Shanmugam, G., 1997, The Bouma sequence and the turbidite mind set: Earth Sci. Rev., **42,** 201–229, doi: 10.1016/S0012-8252(97)81858-2.

Šimíček D., and O. Bábek, 2015, Assessing provenance of Upper Cretaceous siliciclastics using spectral γ-ray record: Geologica Carpathica, **66**, 4, 311–329, doi: 10.1515/geoca-2015-0028.

Svendsen, J.B., and N.R. Hartley, 2001, Comparison between outcrop-spectral gamma ray logging and whole rock geochemistry: implications for quantitative reservoir characterization in continental sequences: Marine and Petroleum Geology, **18**, 657–670, doi: 10.1016/S0264-8172(01)00022-8.

Talling, P.J., D.G. Masson, E.J. Sumner, and G. Malgesini, 2012. Subaqueous sediment density flows: depositional processes and deposit types: Sedimentology**,** **59**, 7, 1937–2003, doi: 10.1111/j.1365-3091.2012.01353.x.

Vesely, F.F., 2006, Dinâmica sedimentar e arquitetura estratigráfica do Grupo Itararé (Carbonífero-Permiano) no centro-leste da Bacia do Paraná: PhD Thesis, Postgraduate Course in Geology, Universidade Federal do Paraná - UFPR, Curitiba, PR, Brazil. 226 pp.

Vesely, F.F., 2007, Sistemas subaquosos alimentados por fluxos hiperpicnais glaciogênicos: modelo deposicional para arenitos do Grupo Itararé, Permocarbonífero da Bacia do Paraná: Boletim de Geociências da Petrobras, **15**, 7–25.

Vesely, F.F., and M.L. Assine, 2006, Deglaciation sequences in the Permo-Carboniferous Itararé Group Paraná Basin Southern Brazil: Journal of South American Earth Sciences, **22**, 156–168, doi: 10.1016/j.jsames.2006.09.006.

Wilford, J.R., P.N. Bierwirth, and M.A. Craig, 1997, Application of airborne gamma-ray spectrometry in soil/regolith mapping and applied geomorphology: Australian Geological Survey Organisation, AGSO Journal of Australian Geology and Geophysics, **17**, 2, 201–216.

Zavala, C., and S. Pan, 2018, Hyperpycnal flows and hyperpycnites: Origin and distinctive characteristics: Lithologic Reservoirs, **30**, 1, 1–27, doi: 10.3969/j.issn.1673-8926.2018.01.001.

Zielinski, J.P.T., and M.S. Nascimento, 2015, Estratigrafia de Sequências de sucessões sedimentares permianas da borda sudeste da Bacia do Paraná, estado de Santa Catarina: Anais do IX Simpósio Sul-Brasileiro de Geologia, Florianópolis, SC, Brazil.

Miranda, A.D.: research design, acquisition, treatment, gammaspectrometric data analysis and interpretation, writing of manuscript texts related to gammaspectrometry; **Nascimento, M.S.:** research design, sample collection, faciological analysis and interpretation, writing of manuscript texts related to faciological aspects; **Castro, N.A.:** gamma-spectrometric data analysis and interpretation; **Baesso, J.P.:** faciological analysis and interpretation; **Balistieri, P.R.M.N.:** ichnological analysis and interpretation.

Received on February 10, 2023 / Accepted on April 18, 2023